AD-A169 485 THE ANALYSIS OF EXPERIMENTAL MEASUREMENTS ON LIQUID REGENERATIVE GUNS(U) ARMY BALLISTIC RESEARCH LAB ABERDEEN PROVING GROUND MD T P COFFEE MAY 86 1/1

UNCLASSIFIED BRL-TR-2731 F/G 19/6 NL

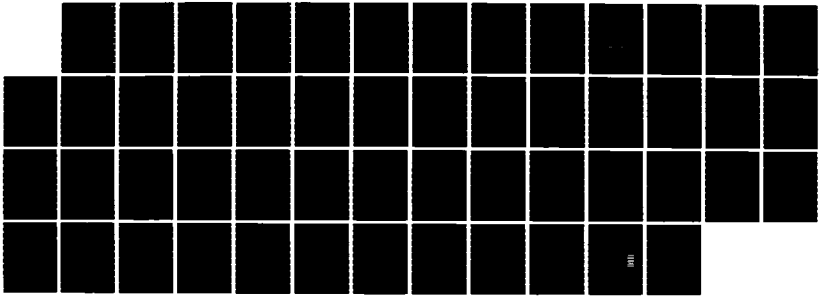

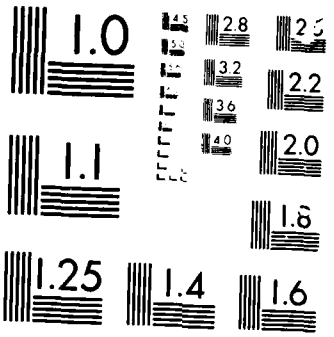
1.0
1.1
1.25
1.4
1.6
1.8
2.0
2.2
2.8
3.2
3.6
4.0

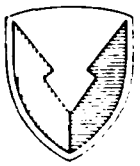

AD

TECHNICAL REPORT BRL-TR-2731

THE ANALYSIS OF EXPERIMENTAL MEASUREMENTS ON LIQUID REGENERATIVE GUNS

Terence P. Coffee

May 1986

US ARMY BALLISTIC RESEARCH LABORATORY
ABERDEEN PROVING GROUND, MARYLAND

Destroy this report when it is no longer needed.
Do not return it to the originator.

Additional copies of this report may be obtained from the National Technical Information Service, U. S. Department of Commerce, Springfield, Virginia 22161.

The findings in this report are not to be construed as an official Department of the Army position, unless so designated by other authorized documents.

The use of trade names or manufacturers' names in this report does not constitute indorsement of any commercial product.

UNCLASSIFIED

SECURITY CLASSIFICATION OF THIS PAGE *(When Data Entered)*

REPORT DOCUMENTATION PAGE		READ INSTRUCTIONS BEFORE COMPLETING FORM
1. REPORT NUMBER Technical Report BRL-TR-2731	2. GOVT ACCESSION NO.	3. RECIPIENT'S CATALOG NUMBER
4. TITLE *(and Subtitle)* THE ANALYSIS OF EXPERIMENTAL MEASUREMENTS ON LIQUID REGENERATIVE GUNS		5. TYPE OF REPORT & PERIOD COVERED 6. PERFORMING ORG. REPORT NUMBER
7. AUTHOR(s) Terence P. Coffee		8. CONTRACT OR GRANT NUMBER(s)
9. PERFORMING ORGANIZATION NAME AND ADDRESS US Army Ballistic Research Laboratory ATTN: SLCBR-IB Aberdeen Proving Grond, MD 21005-5066		10. PROGRAM ELEMENT, PROJECT, TASK AREA & WORK UNIT NUMBERS 1L263637D155
11. CONTROLLING OFFICE NAME AND ADDRESS US Army Ballistic Research Laboratory ATTN: SLCBR-DD-T Aberdeen Proving Ground, MD 21005-5066		12. REPORT DATE May 1986 13. NUMBER OF PAGES 48
14. MONITORING AGENCY NAME & ADDRESS*(if different from Controlling Office)*		15. SECURITY CLASS. *(of this report)* Unclassified 15a. DECLASSIFICATION/DOWNGRADING SCHEDULE

16. DISTRIBUTION STATEMENT *(of this Report)*

Approved for public release; distribution unlimited.

17. DISTRIBUTION STATEMENT *(of the abstract entered in Block 20, if different from Report)*

18. SUPPLEMENTARY NOTES

19. KEY WORDS *(Continue on reverse side if necessary and identify by block number)*

liquid monopropellant	fuel injection
regenerative gun	discharge coefficient
lumped parameter model	droplet burning

20. ABSTRACT *(Continue on reverse side if necessary and identify by block number)*

Existing numerical models for regenerative liquid propellant guns involve major simplifications of the processes occurring during the firing cycle. To determine the adequacy of these assumptions, a model is compared with experimental measurements. The differences can be explained in terms of the injection of the fuel through the piston and the liquid accumulation in the

DD FORM 1 JAN 73 1473 EDITION OF 1 NOV 65 IS OBSOLETE

UNCLASSIFIED

SECURITY CLASSIFICATION OF THIS PAGE *(When Data Entered)*

20. ABSTRACT (Con't)

combustion chamber. From the experimental profiles, input values are derived that can be used in the gun code and that better model the liquid injection and accumulation.

TABLE OF CONTENTS

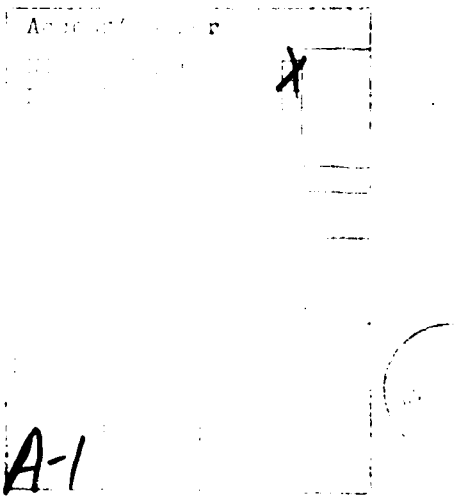

LIST OF FIGURES

LIST OF FIGURES (CON'T)

I. INTRODUCTION

In this report we consider annular liquid propellant guns (see Figure 1). The regenerative piston surrounds a central bolt. As the piston begins to move, it opens up a small annular vent between the piston and the bolt. The bolt is tapered, so the vent opening becomes gradually larger. There is a long straight section where the vent area is constant, and finally a back taper to slow down the piston. The top of Figure 1 shows the gun before firing, and the bottom of the figure shows the gun after firing.

The liquid jet enters the combustion chamber at high speed. After some delay, the jet breaks up into droplets. The droplets formed may break up further or coalese. The propellant will eventually ignite, and may burn as individual droplets or as an envelope flame. Gas recirculation will further affect the spray combustion.

The fluid flows from the combustion chamber into the gun tube. For liquid guns, there is typically a large area change between the chamber and the tube. This cannot be ignored, as is often done in solid propellant gun codes.

Regenerative liquid propellant gun codes[1-4] involve a number of simplifying assumptions. As the codes consider only lumped parameter or at most one-dimensional regions, higher dimensional effects are ignored. Besides this, there are three major areas of uncertainty. First is the

---

[1] Pagan, G., and Izod, D.C.A., "Regenerative Liquid Propellant Gun Modelling," Proceedings of the Seventh International Symposium on Ballistics, The Hague, The Netherlands, April 1983.

[2] Cushman, P.G., "Regenerative Liquid Propellant Gun Simulation User's Manual," GE Report 84-POD-004, December 1983.

[3] Gough, P.S., "A Model of the Interior Ballistics of Hybrid Liquid-Propellant Guns," Final Report, Contract DAAK11-82-C-1054, PGA-TR-83-4, September 1983.

[4] Coffee, T.P., "A Lumped Parameter Code for Regenerative Liquid Propellant Guns," Technical Report BRL-TR-2703, December 1985.

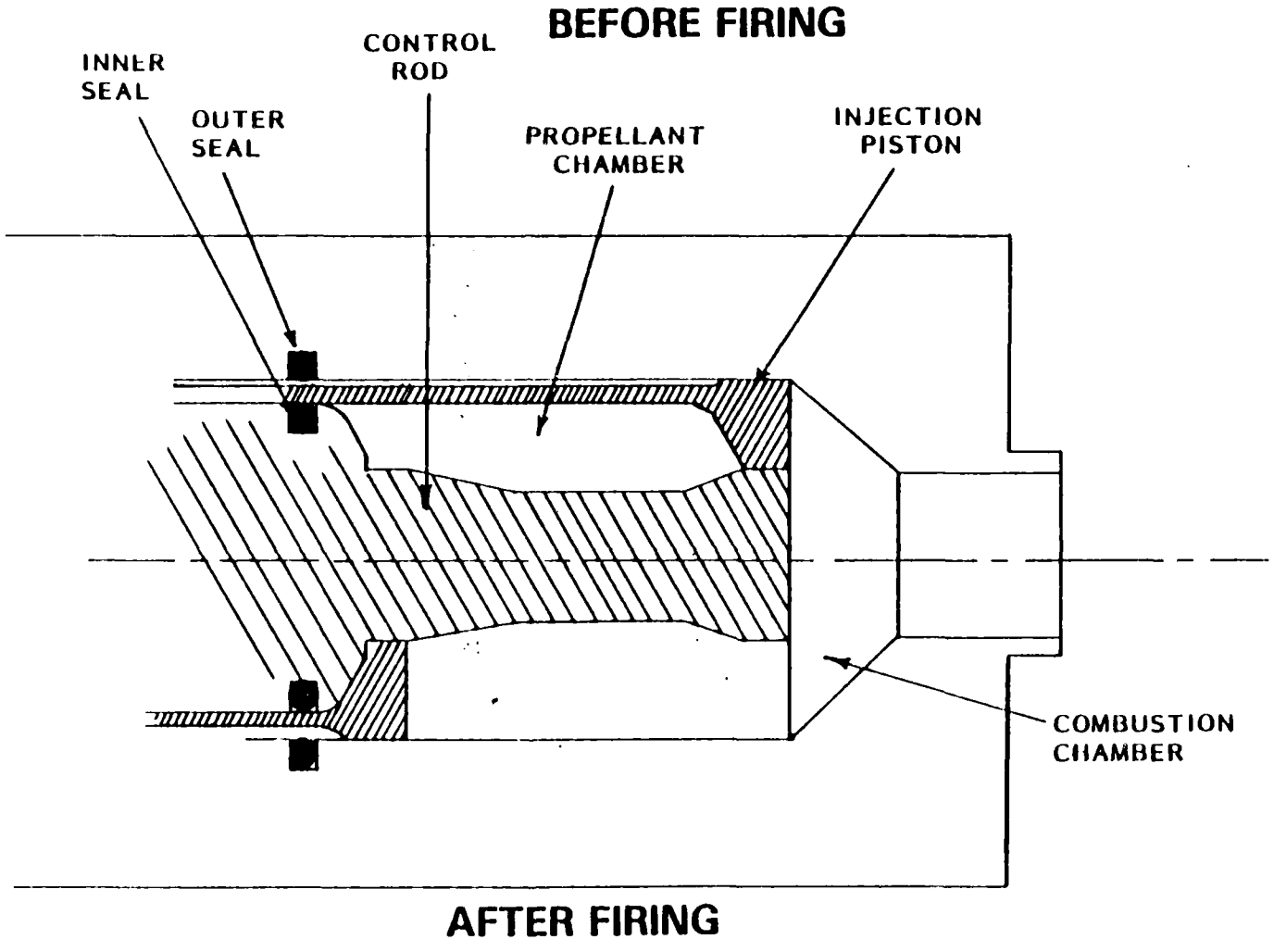

Figure 1. A Regenerative Liquid Propellant Gun with an Annular Piston.

injection of the liquid propellant through the orifice in the face of the piston into the combustion chamber. This is approximated as steady state Bernoulli flow. The various possible loss terms (entrance losses, frictional losses, inertial effects, etc.)are lumped into the discharge coefficient. This is treated as an adjustable parameter, and varied so as to obtain the desired chamber pressure.

Second is the liquid accumulation in the combustion chamber. For lack of further information, we usually assume that the liquid combusts instantaneously when it enters the combustion chamber, although simple droplet burning models are also available.

Last, there is the fluid flow from the combustion chamber into the gun tube. This flow is approximated by steady state Bernoulli or isentropic flow, again with an adjustable discharge coefficient to take into account unknown loss terms. This coefficient is normally set equal to one.

Recently, a set of experimental measurements has been made on a 30-mm regenerative liquid propellant gun.[5] [6] These include the liquid reservoir pressure, the combustion chamber pressure, the piston travel, and the projectile velocity. The pressure traces have been filtered (20 Megahertz band pass filter) to remove the acoustic oscillations. A number of cases have been measured for the 2/3 charge and the 1/3 charge. The gun has not yet been fired with a full charge.

From the engineering drawings, the initial reservoir volume for the 1/3 charge case is 83.3 cm^3, and the initial volume for the 2/3 charge case is 171.1 cm^3. These values are used in this report. An actual measurement of the liquid injected into the reservoir indicates a volume of 79 cm^3 for the

---

[5] Knapton, J.D., Watson, C., and DeSpirito, J., "Test Data from a Regenerative Sheet Injector Type of Liquid Propellant Gun," 22nd JANNAF Combustion Meeting, October 1985.

[6] Watson, C., DeSpirito, J., Knapton, J.D., and Boyer, N., "A Study on High Frequency Pressure Oscillations Observed in a 30-mm Regenerative RLG," 22nd JANNAF Combustion Meeting, October 1985.

1/3 charge case.[7] The difference may be partially due to ullage in the liquid reservoir. More likely, the transducer block is slightly forward of its theoretical position, leading to a reduced volume.

In this article we consider the data from 2 cases for each charge weight. The pressure was recorded at three locations in the combustion chamber. The pressure transducer at location J is initially in the combustion chamber. The other transducers are initially in the grease column between the outside of the piston and the chamber wall. The transducer at location C is uncovered after the piston has moved about 2.0 centimeters. The transducer at location A is only exposed after the piston has moved 4.1 centimeters. Data from the latter two locations are only shown after the transducers are in the combustion chamber. Not all the data was recorded successfully for each case.

Our goal is to obtain information about the three processes discussed above. Since no measurements were taken of the gun tube pressures, information about the fluid injection into the tube is not available. In this paper we assume that the flow is isentropic with a discharge coefficient of one.

II. EXPERIMENTAL DATA

Figures 2 and 3 shows the experimental chamber pressures for the 2/3 charge cases (round 8 and round 14). The pressures are given for all three pressure transducers in the chamber. For comparison, the results of a lumped parameter model are also given.[4] The model assumes instantaneous burning in the combustion chamber and the discharge coefficient has been set equal to 0.85 to match the experimental chamber pressure (at transducer J). All the model results in this report assume isentropic flow into the gun tube (discharge coefficient equal to one), a modified Lagrange pressure distribution in the gun tube (which takes into account the large fluid

---

[7] Watson, C., Ballistic Research Laboratory, private communication.

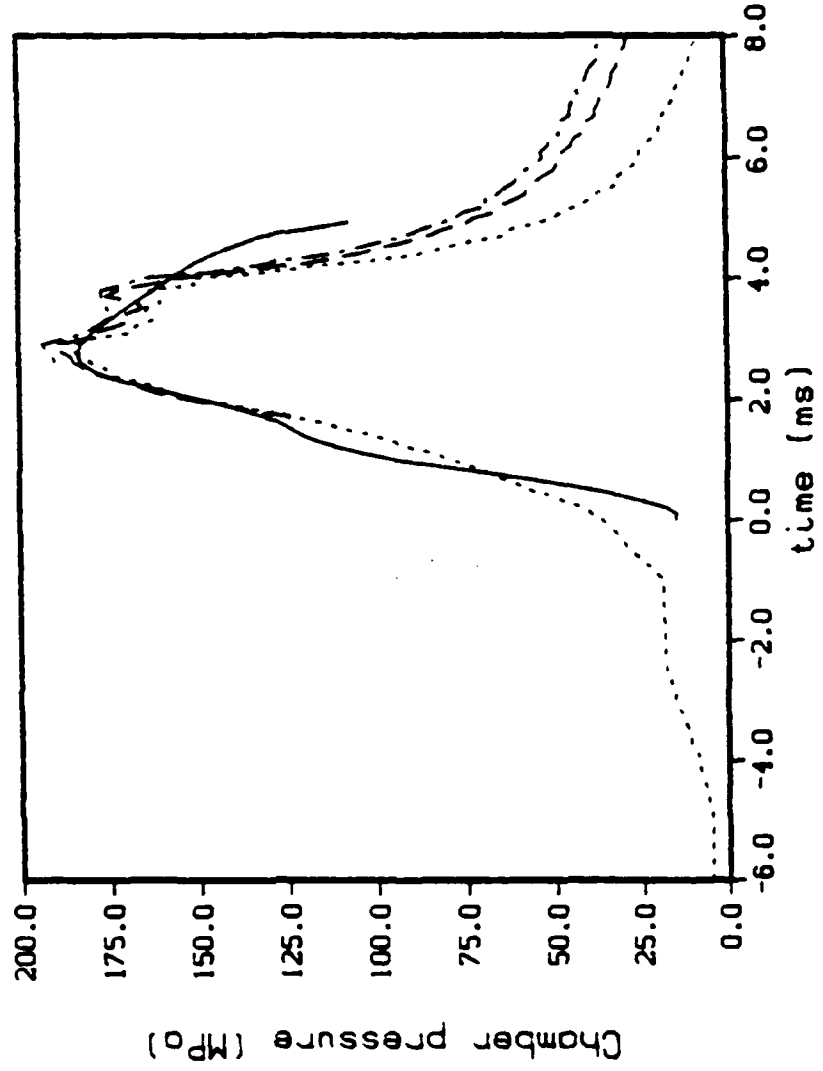

Figure 2. Chamber Pressure for Round 8 (2/3 charge). Model with $C_D = 0.85$ and Instantaneous Burning (line). Experimental curves J (dot), C (dash), and A (dot-dash).

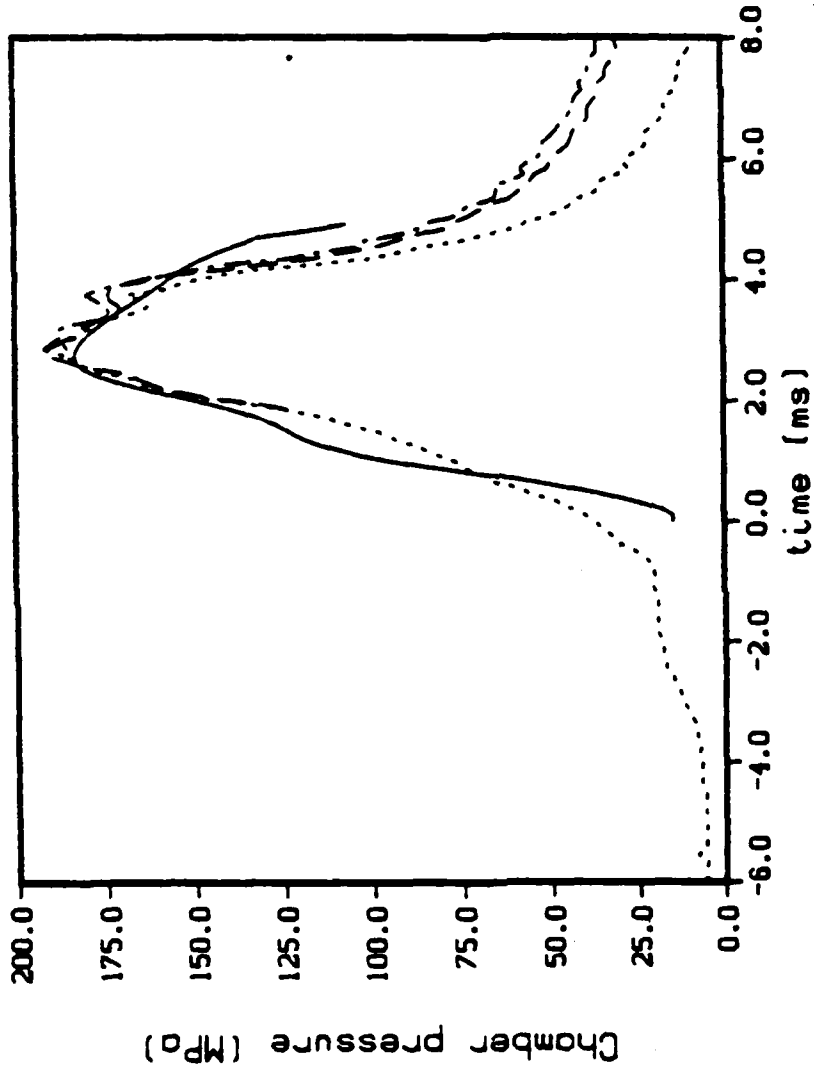

Figure 3. Chamber Pressure for Round 14 (2/3 charge). Model with C_D = 0.85 and Instantaneous Burning (line). Experimental Curves J (dot), C (dash), and A (dot-dash).

velocity in the throat of the gun tube), and simple approximations for the heat loss to the gun tube and the air shock in front of the projectile. For purposes of comparison, the experimental curves have been shifted in time so that the model and curve J reach the shot start pressure (68 MPa) at the same time.

There is good agreement between the two firings and among the three pressure transducers. Late in the firing cycle, the data shows a pressure gradient in the combustion chamber. The chamber is by now too large for a rapid enough pressure equilibrium. The present generation of models, which all treat the combustion chamber as a homogeneous region, cannot model this behavior.

The model curve shows fair agreement during the rapid pressure rise. The agreement is very poor during the early part of the firing cycle, and is not very good at later times in the cycle.

Figure 4 shows the piston travel for round 8. This data was not successfully recorded for round 14. The experiment shows earlier piston travel compared to the pressure rise, indicating that liquid is being injected into the combustion chamber before combustion has really started. The model shows a slightly longer piston travel than the experiment. This is because the piston is assumed in the code to be infinitely thin. The effect of a more detailed piston model was judged to be minor. In order to preserve the proper initial liquid reservoir volume, the piston travel does have to be slightly longer than in the actual gun.

Figures 5, 6, and 7 show the analogous data for the 1/3 charge cases (round 2 and round 9). The model used the same value for the discharge coefficient (0.85) in order to see if the same parameters could represent both the 2/3 charge and the 1/3 charge cases. In this case, the model pressure shows an unusual two humped pattern. The first pressure maximum occurs when the vent opening is still small. Since the liquid reservoir volume is small, the liquid pressurizes rapidly, and reaches a pressure well above that predicted by the hydraulic difference between the two chambers. When the vent area increases, this overpressure is relieved. The resulting

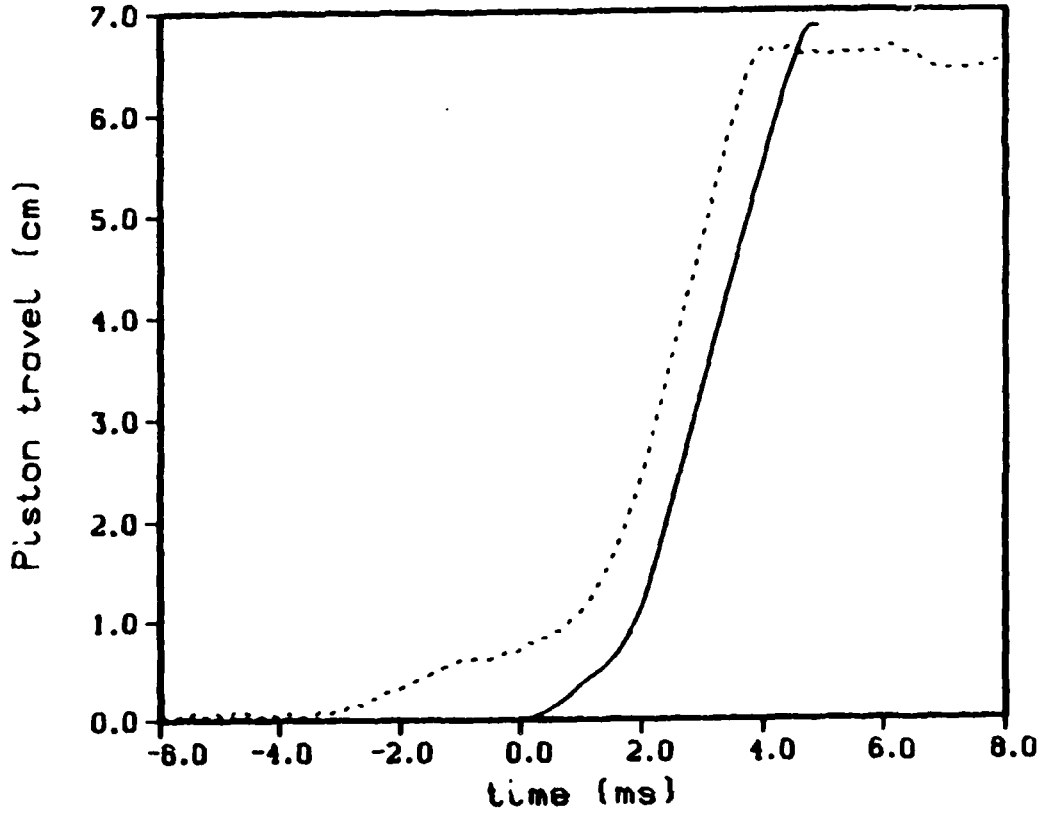

Figure 4. Piston Travel for Round 8 (2/3 charge). Model with C_D = 0.85 and Instantaneous Burning (line). Experimental Curve (dot).

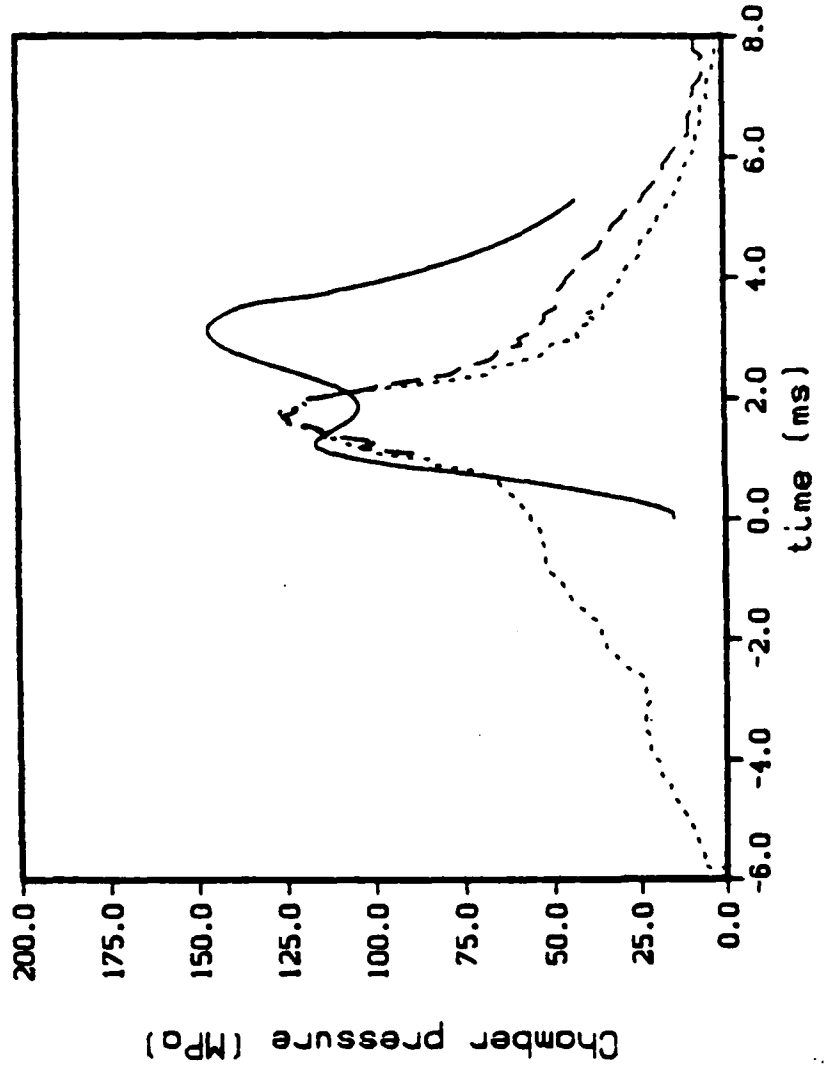

Figure 5. Chamber Pressure for Round 2 (1/3 charge). Model with C_D = 0.85 and Instantaneous Burning (line). Experimental Curves J (dot) and C (dash).

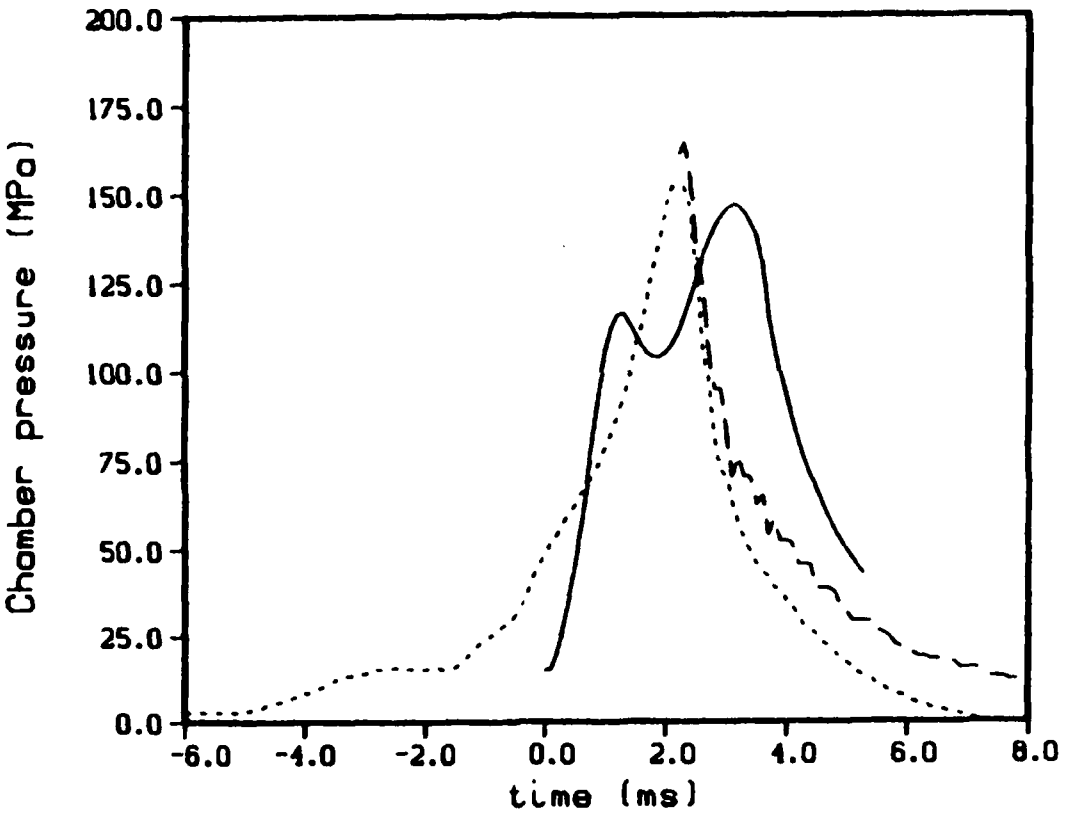

Figure 6. Chamber Pressure for Round 9 (1/3 charge). Model with C_D = 0.85 and Instantaneous Burning (line). Experimental Curves J (dot) and C (dash).

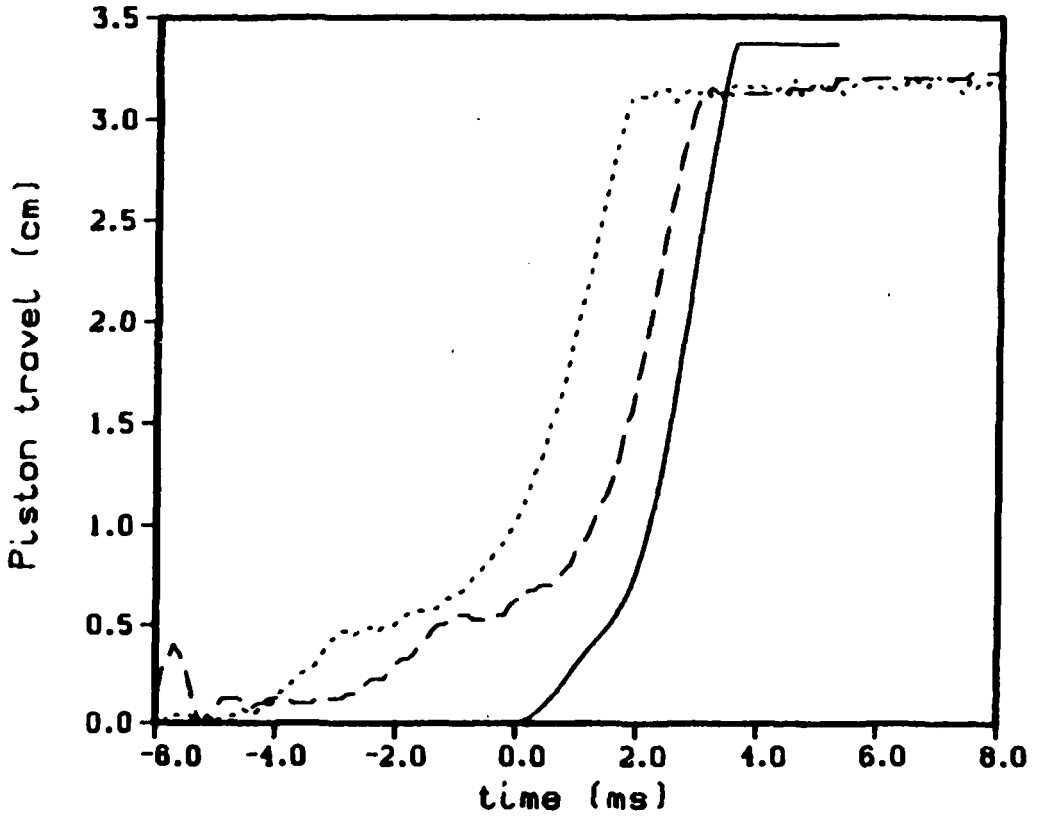

Figure 7. Piston Travel for Round 2 and Round 9 (1/3 charge). Model with C_D = 0.85 and Instantaneous Burning (line). Experimental Curves (dot, dash).

lower liquid pressure leads to a lower injection rate, and the chamber pressure falls. Finally, a more normal pressure peak is obtained. For this particular case, the double hump is an artifact, due to the assumption of instantaneous burning. In other experiments, this type of pattern has been observed, indicating that in some cases the effect does occur.

Round 9 shows a much larger peak pressure than round 2, and a lower pressure in the early part of the firing cycle. Apparently, during round 2, the liquid began combusting earlier, leading to a higher early pressure and a lower peak pressure.

Experiments for low pressure ignition of liquid propellants show a large variation in ignition times for the same heating rate.[8] Also, erratic ignition behavior has occurred in other fixtures.[9] Since the pressure curves show differences for early times, the difference in peak pressures is probably due to differences in the ignition. Different crash rings were used in the two tests, which could effect the ignition.

Both the experimental piston travels (Figure 7) indicate liquid accumulation during the early part of the firing cycle.

III. DATA ANALYSIS

The mass flux through the piston is assumed to obey the steady state Bernoulli law

$$\text{mass flux} = C_D A_V \sqrt{2 g_o \rho_l (P_1 - P_3)} \qquad (1)$$

---

[8] Miller, M., Ballistic Research Laboratory, private communication.

[9] Reever, K.P., "Operating Manual and Final Test Report for 30-mm BRL Regenerative Liquid Propellant Test Fixture," General Electric Ordnance Systems Division Report, Contract No. DAAK11-83-C-0007.

where C_D is the discharge coefficient, A_V is the vent area, g_o is a conversion constant, ρ_l is the liquid density, p_l is the liquid pressure, and p_3 is the combustion chamber pressure. The pressures and vent area are known. The liquid density can be computed from the equation of state.[4] Now integrate both sides over a time interval. The left side is just the difference of the liquid masses in the reservoir at the two times. The right side can be approximated using numerical integration. An average value of C_D over the time interval is obtained.

The mini-transducers used in the liquid propellant chamber are known to suffer from inaccuracies. Also, small errors in each pressure can lead to large errors in the pressure difference. So the liquid pressure is approximated by the chamber pressure times the hydraulic difference (for this piston, 1.4746). This is a good approximation, and would be exact for an incompressible liquid. The integrations are performed over time intervals corresponding to equal piston displacements (0.2 cm).

Results are given in Figure 8 for the 2/3 charge. At early times, the vent opening is very small, and the discharge coefficients are large. As the piston moves and the vent area increases, C_D drops rapidly, and then slowly increases to large values again. Figures 9 and 10 show the results for the 1/3 charge. For purposes of comparison, Figure 11 shows the three experimental curves for position J. The curves are qualitatively similar. It is not yet known if the delay in reaching a high discharge coefficient is due to inertial effects (delay in accelerating the liquid to the steady state values) or to a change in steady state conditions (such as Reynold's number effects).

It is also possible to compute the liquid accumulation, using conservation of mass and energy. At any given time, we know how much liquid is still in the reservoir. The energy of the liquid is assumed to be the chemical energy times the mass. The balance of the original charge is in the combustion chamber/gun tube. The total energy and mass in this region is hence known. We assume that when the liquid combusts, it immediately releases all of its chemical energy.

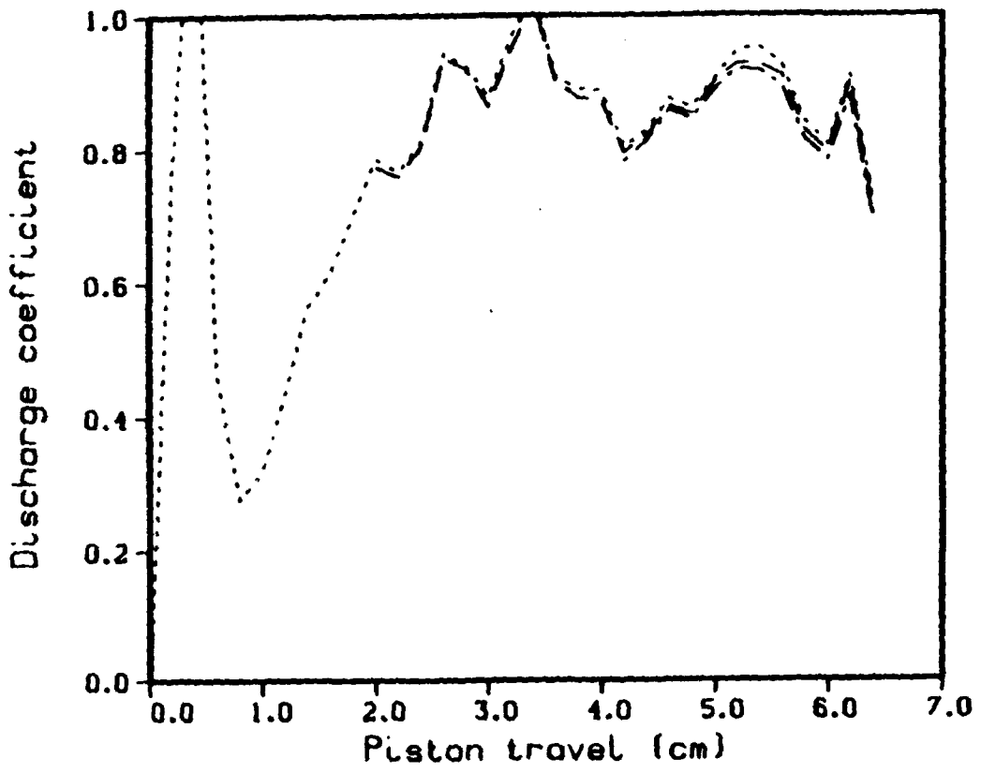

Figure 8. Experimental Discharge Coefficients for Round 8 (2/3 charge). Position J (dot), C (dash), and A (dot-dash).

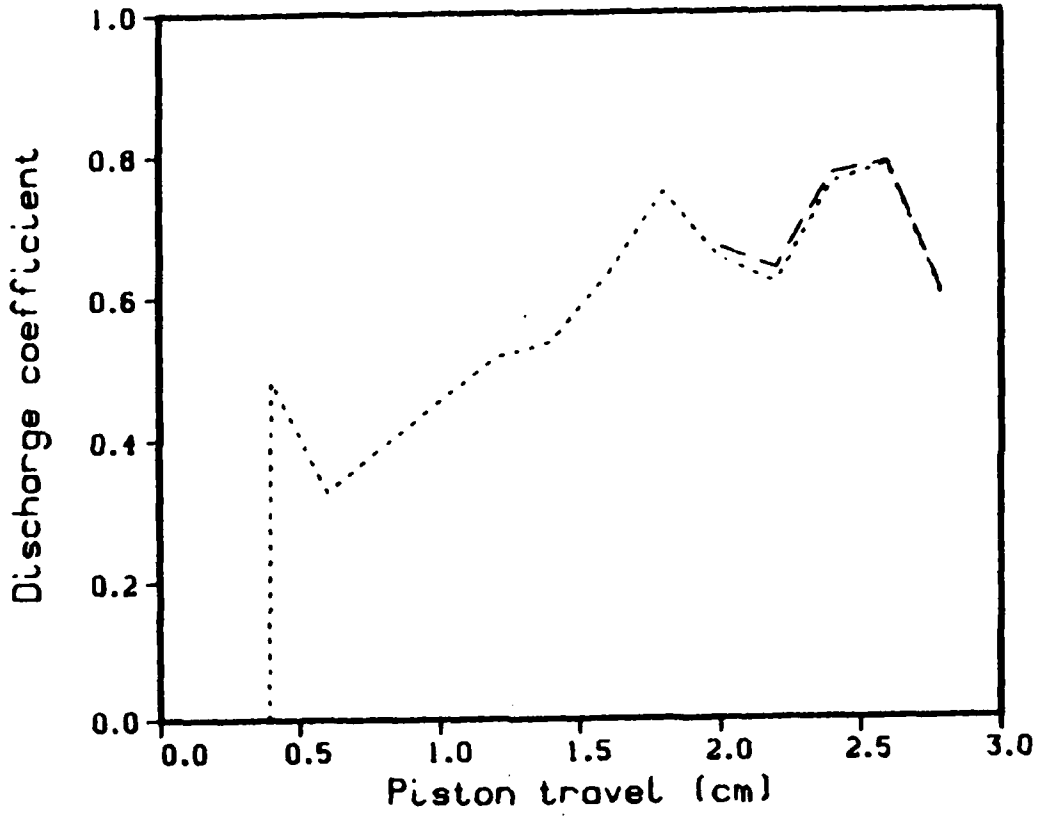

Figure 9. Experimental Discharge Coefficients for Round 2 (1/3 charge). Position J (dot) and C (dash).

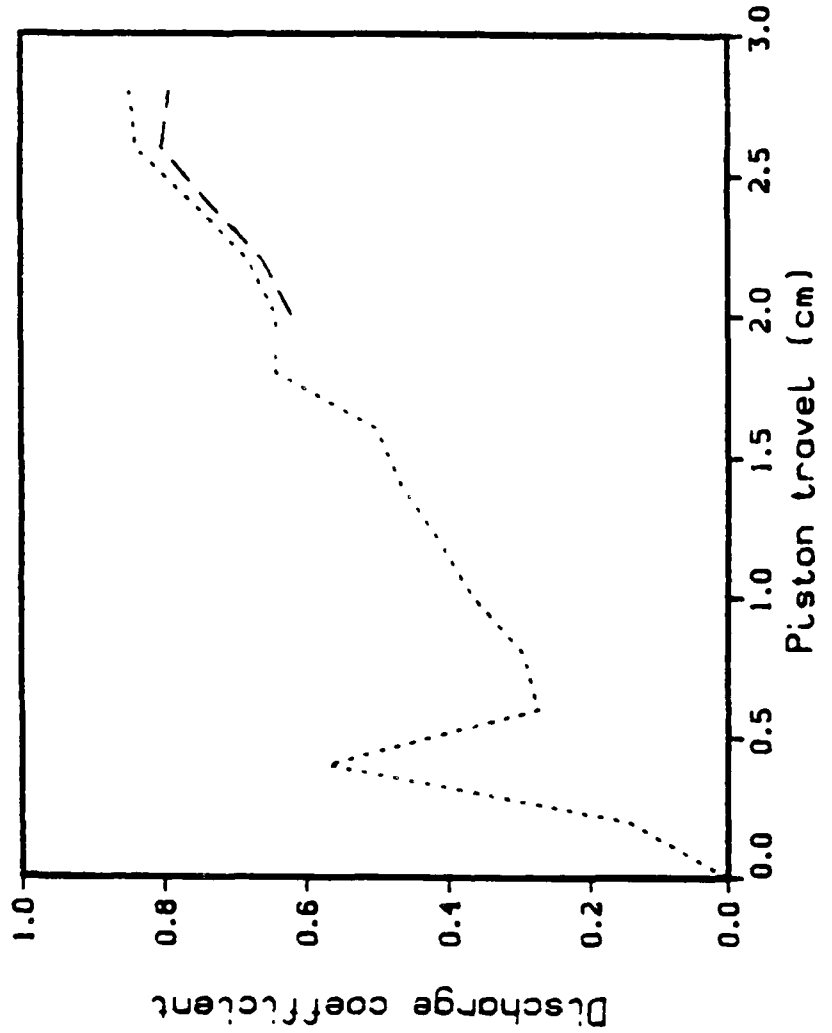

Figure 10. Experimental Discharge Coefficients for Round 9 (1/3 charge). Position J (dot) and C (dash).

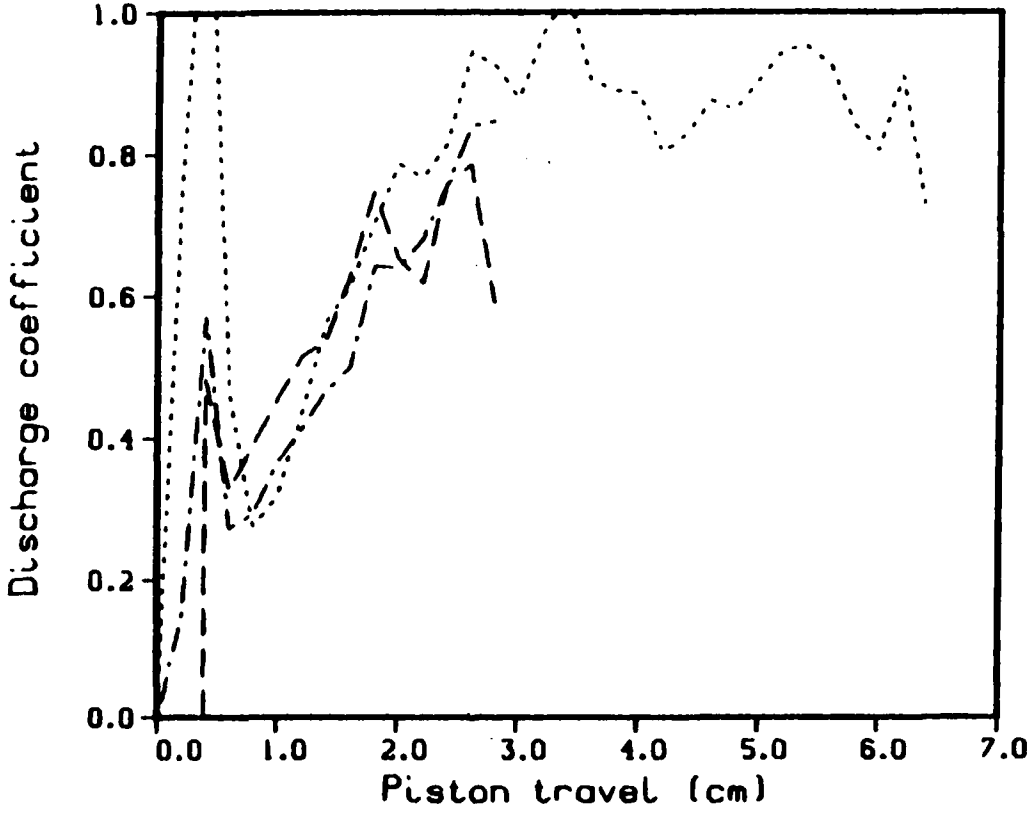

Figure 11. Experimental Discharge Coefficients for Position J. Round 8 (dot), Round 2 (dash), and Round 9 (dot-dash).

The total energy in the combustion chamber/gun tube must equal the chemical energy of the liquid, the internal energy of the gas, and the kinetic energy of the piston, the projectile, and the gas. Energy loss terms (heat loss to the tube, air shock, frictional resistance, etc.) are ignored.

The experimental projectile velocity is noisy near the beginning of the firing cycle. So we assume that the velocity is zero if the chamber pressure is less than the shot start pressure (68 MPa). Also, the velocity measurement usually breaks down before the projectile exits the tube. In this case, the projectile velocity is extrapolated.

The tube pressure is assumed to be equal to the chamber pressure. This is accurate for early times, before the projectile is moving rapidly. The piston velocity is obtained by numerical differentiation. The projectile travel is obtained by numerical integration.

From the piston travel and projectile travel, the volumes of the combustion chamber and the gun tube are computed. Also, the kinetic energy of the piston, the kinetic energy of the projectile, and the kinetic energy of the fluid in the tube (assuming a Lagrange distribution) can be calculated. The liquid density can also be calculated from the equation of state.

We can now set up six equations involving the combustion chamber/gun tube; total energy

$$E_T = e_L M_L + e_G M_G \tag{2}$$

total mass

$$M_T = M_L + M_G \tag{3}$$

total volume

$$V_T = V_L + V_G \tag{4}$$

internal energy of the gas (Noble-Abel equation)

$$e_G = p_3 (1 - b\rho_G) / \rho_G (\gamma - 1) \tag{5}$$

liquid density

$$\rho_L = M_L/V_L \tag{6}$$

and gas density

$$\rho_G = M_G/V_G \, . \tag{7}$$

There are six unknowns; liquid mass, gas mass, liquid volume, gas volume, gas density, and gas internal energy. After some algebra,

$$M_L = \frac{\rho_L E_T (\gamma - 1) + \rho_L M_T p_3 b - p_3 V_T \rho_L}{\rho_L e_L (\gamma - 1) + \rho_L p_3 b - p_3} \, . \tag{8}$$

Results are given in Figures 12-14. For early times, the three cases are almost identical. They all show a significant liquid accumulation. The round 9 case (Figure 14) is different from the other two. Here the liquid

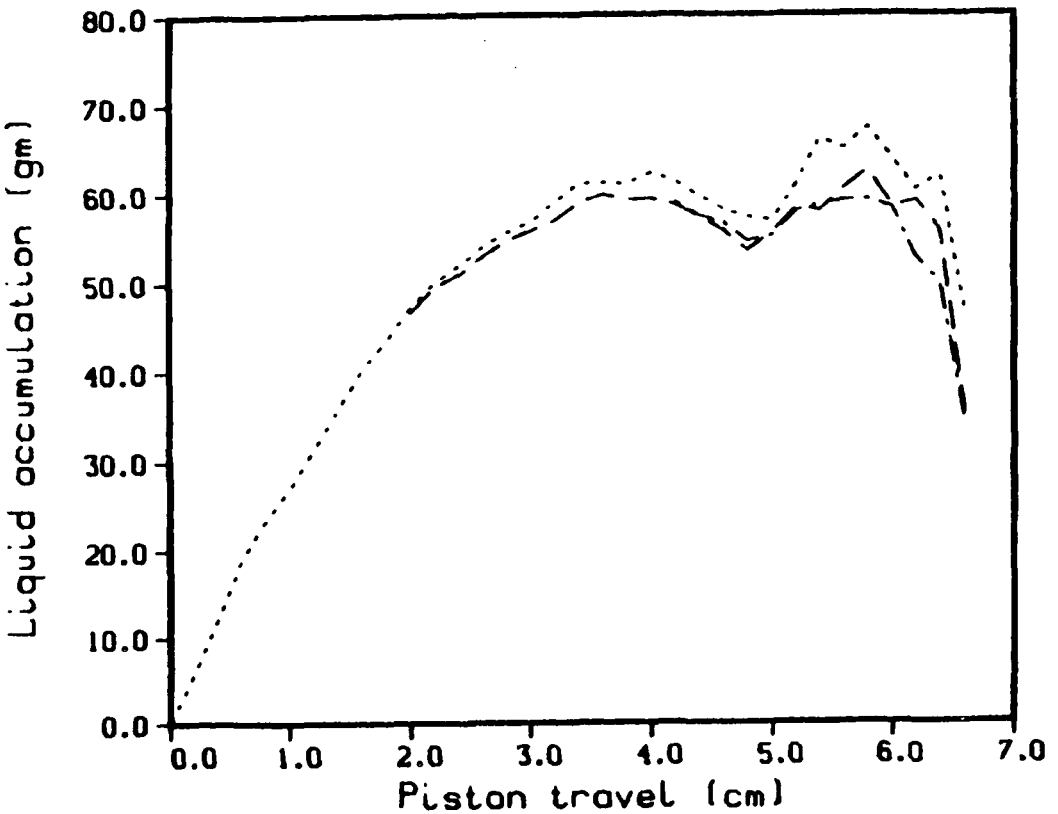

Figure 12. Experimental Liquid Accumulation for Round 8 (2/3 charge). Position J (dot), C (dash), and A (dot-dash).

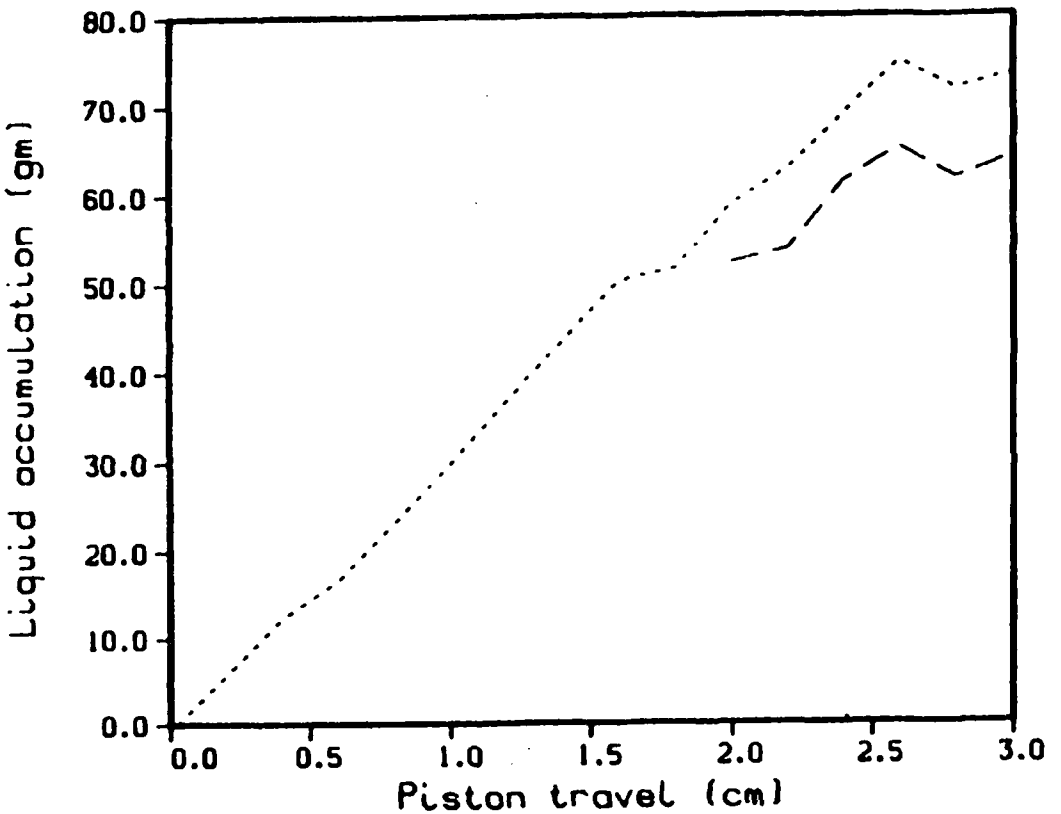

Figure 13. Experimental Liquid Accumulation for Round 2 (1/3 charge). Position J (dot) and C (dash).

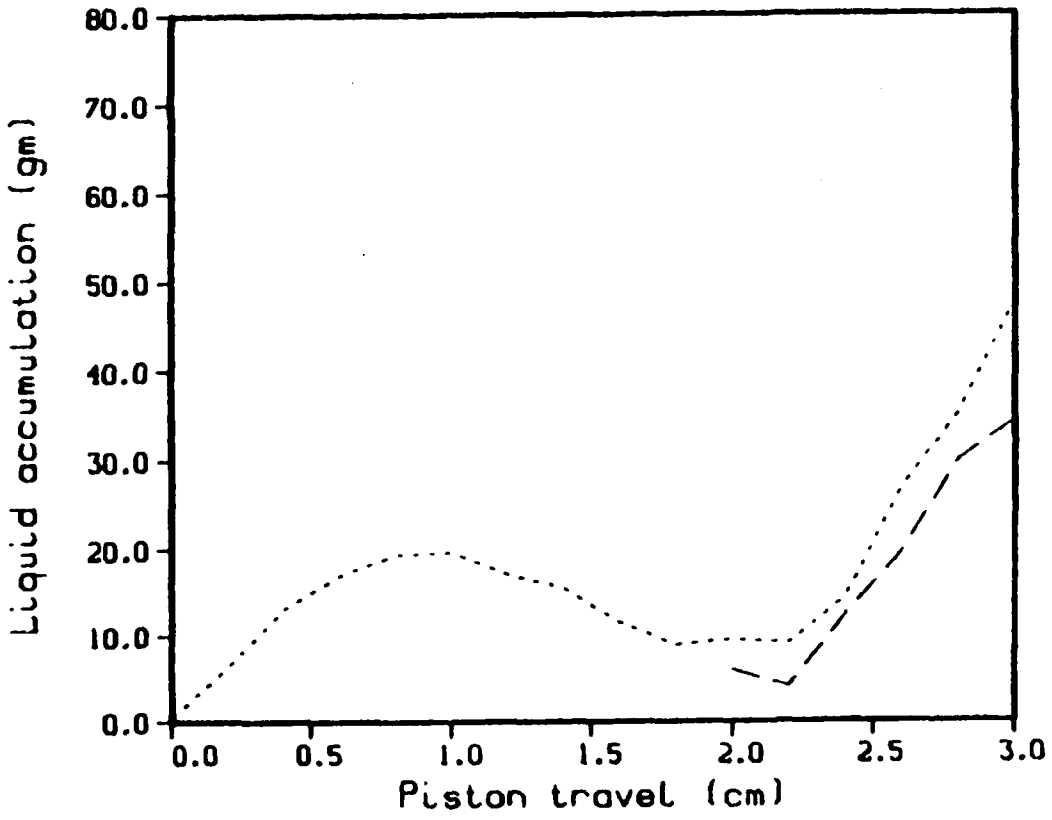

Figure 14. Experimental Liquid Accumulation for Round 9 (1/3 charge). Position J (dot) and C (dash).

burns more rapidly, leading to a drop in the liquid accumulation. At later times the injection rate becomes large enough to again build up the accumulation. For the other two cases, the liquid accumulation builds steadily throughout the piston travel.

Ignoring the lower pressure in the gun tube leads to an underestimate of the liquid accumulation. Ignoring the loss terms leads to an overestimate. If the liquid is heated substantially before combustion occurs, the accumulation will be overestimated. Also, the liquid accumulation is sensitive to errors in the pressure measurements. But the data does show a large accumulation of liquid in the chamber/tube for all three cases.

Additional information can be obtained concerning the burning rate. Assume that the liquid accumulation is in the form of uniform size droplets. The diameter d_s of the droplets is chosen to be the Sauter mean diameter. This is the diameter that preserves the surface area of the original accumulation.

The burning rate is given by

$$\text{burning rate} = M_L \, (6/d_s) \, Ap_3{}^B \tag{9}$$

where M_L is the liquid in the chamber/tube, and $Ap_3{}^B$ is the linear burning rate. This rate has been measured by McBratney.[10] [11] Over a given time interval, the burning rate is approximately equal to the change in the mass of the gas. So the Sauter mean diameter can be estimated over a given interval.

---

[10] McBratney, W.F., "Windowed Chamber Investigation of the Burning Rate of Liquid Monopropellants for Guns," ARBRL-MR-03018, April 1980.

[11] McBratney, W.F., "Burning Rate Date, LGP 1843," ARBRL-MR-03128, August 1981.

Figures 15-17 show the Sauter mean diameters. For early times, the diameter is large, indicating rapid liquid accumulation and slow burning. The diameter then drops rapidly, indicating that the liquid is burning much more efficiently. The liquid accumulation still remains high, but this is due to the rapid influx of propellant from the liquid reservoir.

IV. COMPARISONS

Now we will see what effect the above results have on our use of the gun code. We have already examined the results when the code[4] is run with the usual assumptions.

We would like to use the values generated by the inverse code to improve the agreement. The code can be run assuming that the liquid injected into the chamber immediately forms droplets. All the droplets are assumed to have the same diameter. The code allows both the discharge coefficient and the droplet diameter to vary as a function of piston travel.

These values are simply read off from the inverse code until the region is reached where there appears to be random oscillations. The values are then kept constant. The value of C_D that is greater than one is ignored. The final value for the mean diameter is adjusted slightly to match the experimental peak chamber pressure. Table 1 shows the results.

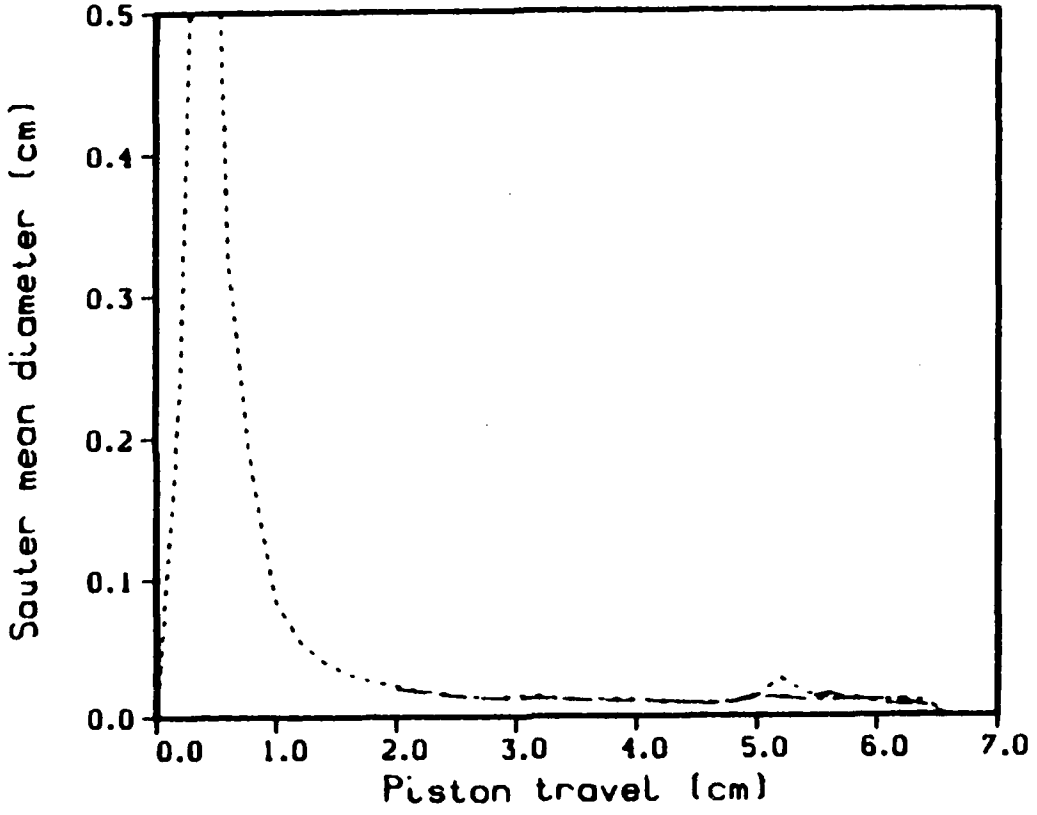

Figure 15. Experimental Sauter Mean Diameter for Round 8 (2/3 charge). Position J (dot), C (dash), and A (dot-dash).

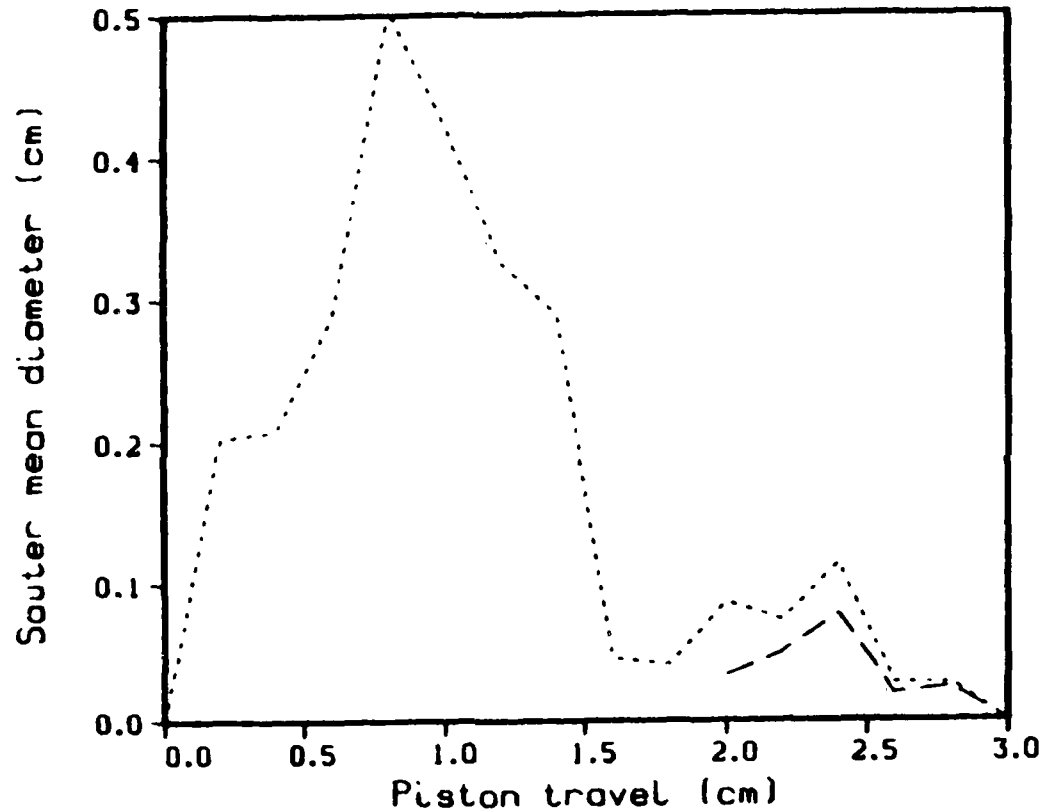

Figure 16. Experimental Sauter Mean Diameter for Round 2 (1/3 charge). Position J (dot) and C (dash).

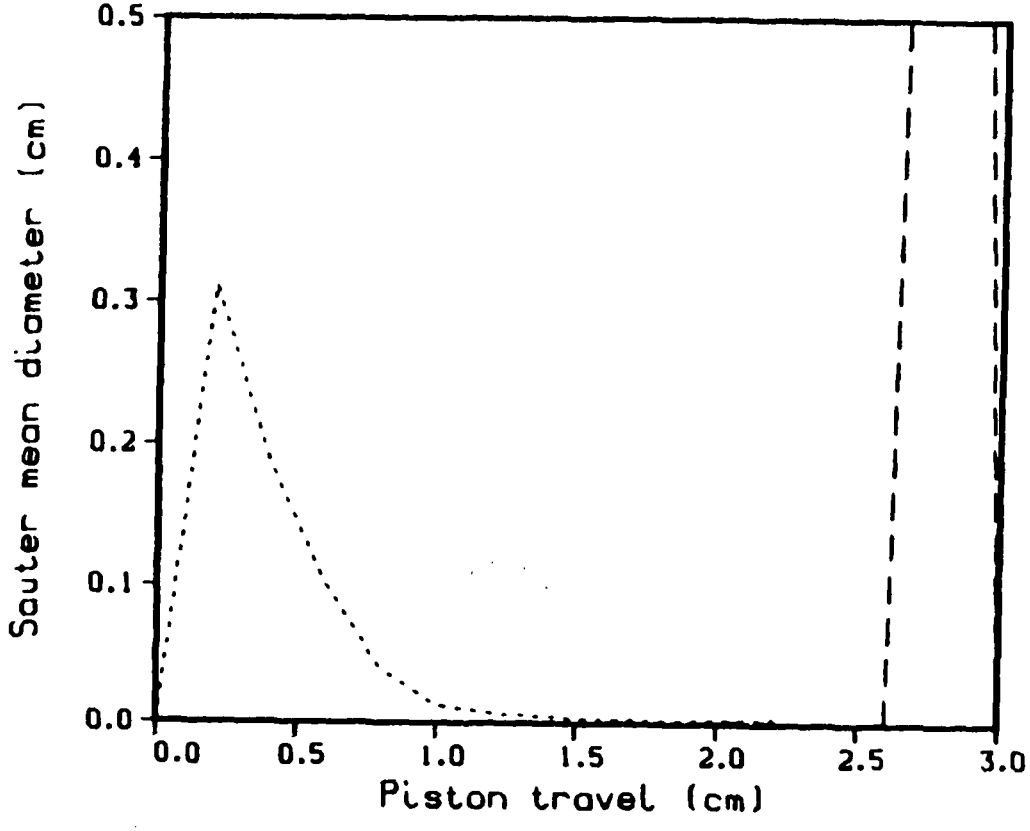

Figure 17. Experimental Sauter Mean Diameter for Round 9 (1/3 charge). Position J (dot) and C (dash).

Table 1. Experimental discharge coefficients and Sauter mean diameters from a 2/3 charge experiment.

Piston travel	C_D	d_s
0.0	.759	.235
0.2	.759	.235
0.4	.759	.874
0.6	.463	.325
0.8	.277	.174
1.0	.318	.085
1.2	.432	.055
1.4	.562	.040
1.6	.615	.031
1.8	.702	.026
2.0	.787	.023
2.2	.767	.019
2.4	.814	.017
2.6	.945	.015
2.8	.926	.013
3.0	.879	.015
3.2		.012
6.848	.879	.012

These values are used in the gun code. The results for the 2/3 charge cases are given in Figures 18, 19, and 20. The agreement is now quite good for both the pressure curves and the piston travel.

The muzzle velocity for the first model is 1088 m/s and for the second is 1080 m/s. So the usual simplifications do not have much effect on the muzzle velocity. The experimental muzzle velocity is between 1000 and 1020 m/s. The lower experimental velocities probably reflect additional loss terms not included in the model.

The liquid accumulation computed by the second model was compared with the values from the inverse code. The agreement is quite good.

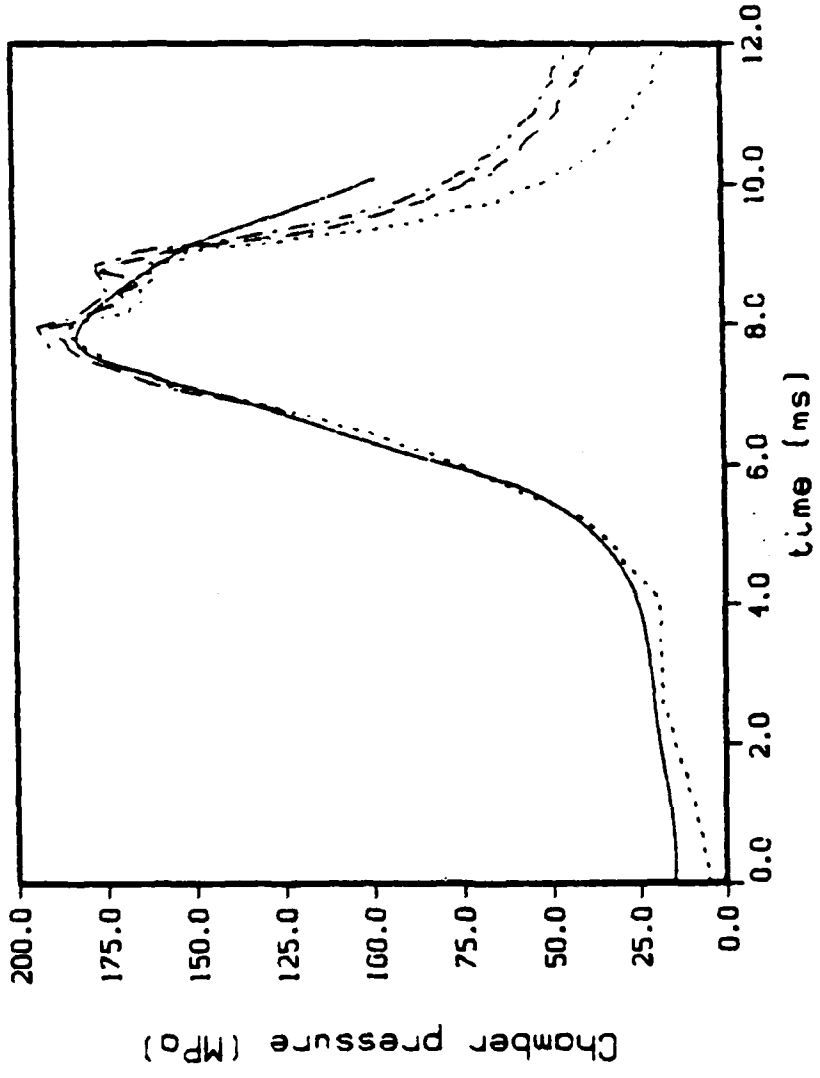

Figure 18. Chamber Pressure for Round 8 (2/3 charge). Model with Experimental C_D and d_s (line). Experimental Curves J (dot), C (dash), and A (dot-dash).

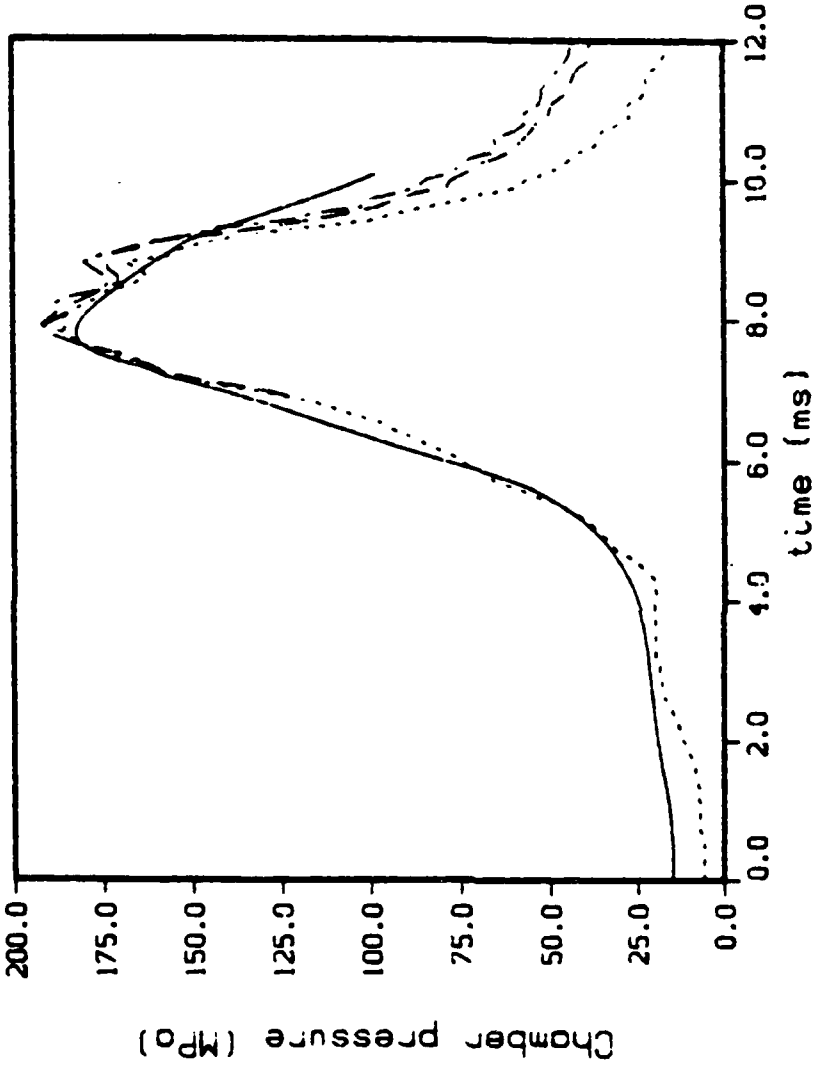

Figure 19. Chamber Pressure for Round 14 (2/3 charge). Model with Experimental C_D and d_s (line). Experimental Curves J (dot), C (dash), and A (dot-dash).

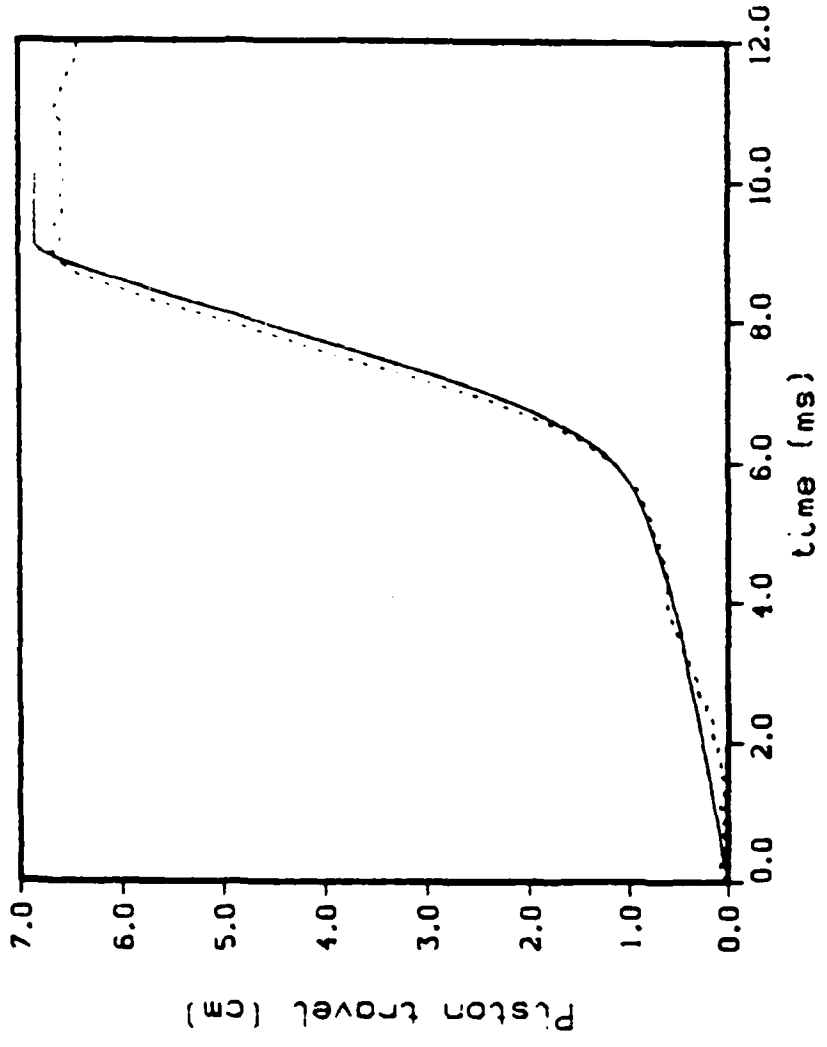

Figure 20. Piston Travel for Round 8 (2/3 charge). Model with Experimental C_D and d_s (line). Experimental Curve (dot).

The values in Table 1, were also used to model the 1/3 charge case. The results are given in figures 21, 22, and 23. The gun code is still in reasonable agreement with the experiments.

V. CONCLUSIONS

We have demonstrated the change in the discharge coefficient during the firing cycle and the accumulation of liquid in the combustion chamber. Both of these effects are important in resolving the details of the firing cycle. But if the proper maximum chamber pressure is achieved, the effect on muzzle velocity is minor.

Knowing the general behavior, we can try to obtain some more fundamental procedure for determining the discharge coefficient and liquid accumulation. Then the performance of the gun could be predicted, instead of having to use the discharge coefficient as an adjustable parameter.

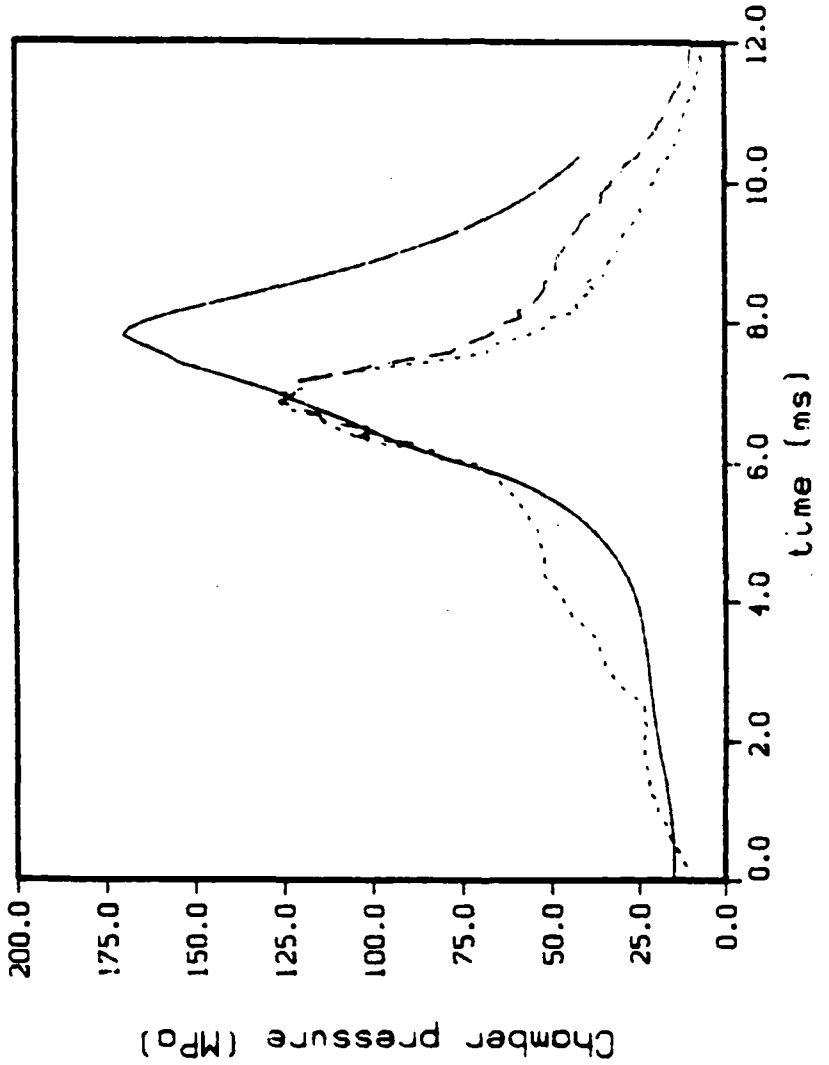

Figure 21. Chamber Pressure for Round 2 (1/3 charge). Model with Experimental C_D and d_s (line). Experimental Curves J (dot) and C (dash).

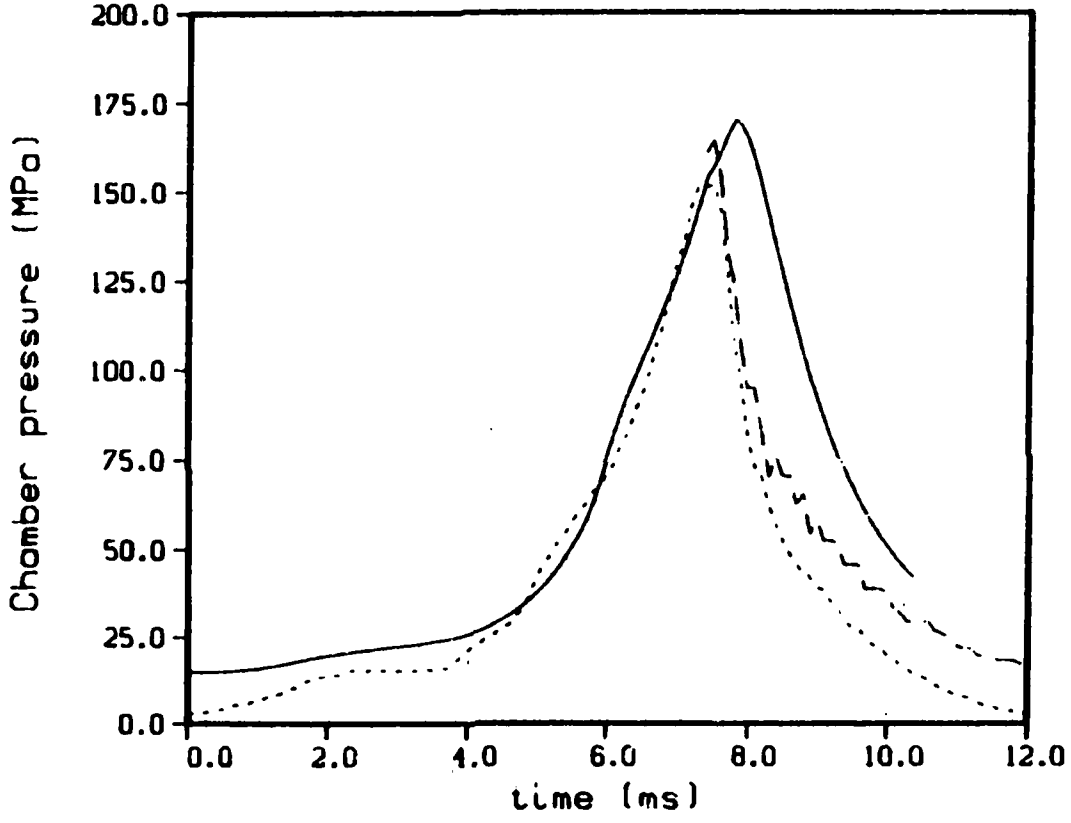

Figure 22. Chamber Pressure for Round 9 (1/3 charge). Model with Experimental C_D and d_s (line). Experimental Curves J (dot) and C (dash).

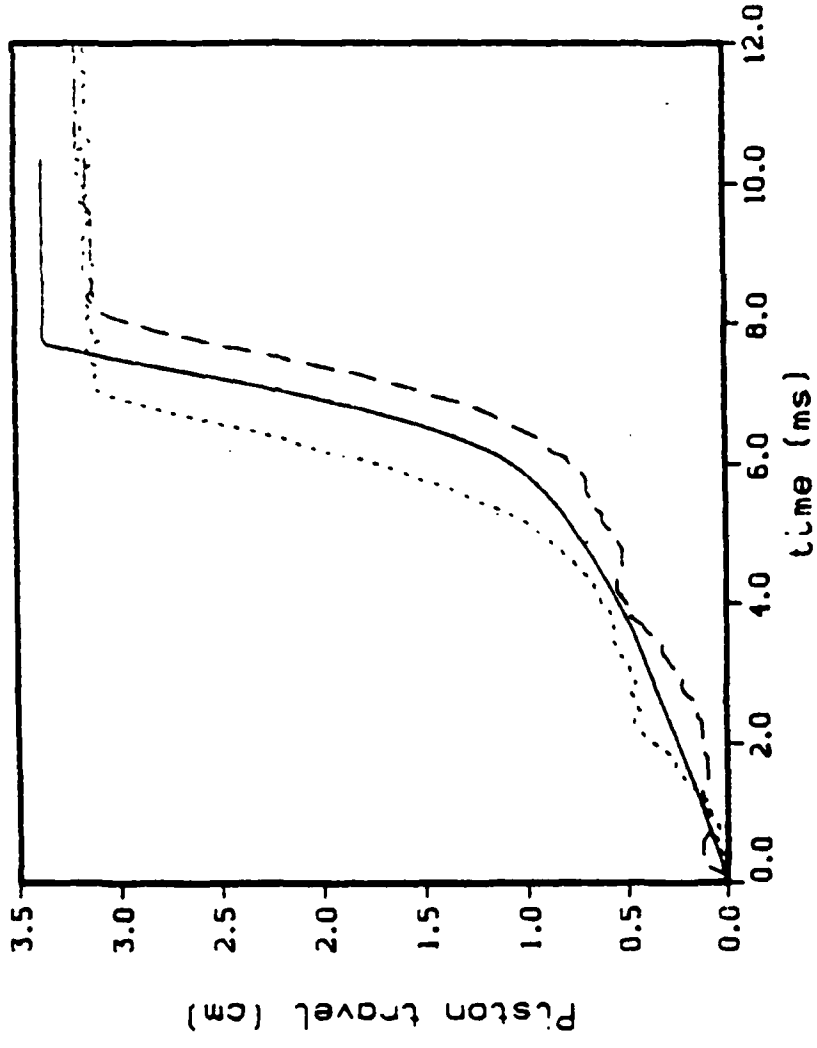

Figure 23. Piston Travel for Round 2 and Round 9 (1/3 charge).
Model with Experimental C_D and d_s (line).
Experimental Curves (dot, dash).

REFERENCES

1. Pagan, G., and Izod, D.C.A., "Regenerative Liquid Propellant Gun Modelling," Proceedings of the Seventh Intrnational Symposium of Ballistics, The Hague, The Netherlands, April 1983.

2. Cushman, P.G., "Regenerative Liquid Propellant Gun Simulation User's Manual," GE Report 84-POD-004, December 1983.

3. Gough, P.S., "A Model of the Interior Ballistics of Hybrid Liquid-Propellant Guns," Final Report, Contract DAAK11-82-C-1054, PGA-TR-83-4, September 1983.

4. Coffee, T.P., "A Lumped Parameter Code for Regenerative Liquid Propellant Guns," Technical Report BRL-TR-2703, December 1985.

5. Knapton, J.D., Watson, C., and DeSpirito, J., "Test Data from a Regenerative Sheet Injector Type of Liquid Propellant Gun," 22nd JANNAF Combustion Meeting, October 1985.

6. Watson, C., DeSpirito, J., Knapton, J.D., and Boyer, N., "A Study on High Frequency Pressure Oscillations Observed in a 30-mm Regenerative RLG," 22nd JANNAF Combustion Meeting, October 1985.

7. Watson, C., Ballistic Research Laboratory, private communication

8. Miller, M., Ballistic Research Laboratory, private communication.

9. Reever, K.P., "Operating Manual and Final Test Report for 30-mm BRL Regenerative Liquid Propellant Test Fixture," General Electric Ordnance Systems Division Report, Contract No. DAAK11-83-C-0007.

10. McBratney, W.F., "Windowed Chamber Investigation of the Burning Rate of Liquid Monopropellants for Guns," ARBRL-MR-03018, April 1980.

11. McBratney, W.F., "Burning Rate Date, LGP 1843," ARBRL-MR-03128, August 1981.

LIST OF SYMBOLS

A_V vent area in the piston face, cm^2

b covolume of the gas, cm^3/g

C_D discharge coefficient for the piston

d_s Sauter mean diameter for the droplet distribution, cm

e_L chemical energy of the liquid, joules/g

e_G internal energy of the gas, joules/g

E_T total energy in the combustion chamber/gun tube, joules

g_o conversion constant, 10^7 g/s^2 -cm-MPa

M_L mass of the liquid in the combustion chamber/gun tube, g

M_G mass of the gas in the combustion chamber/gun tube, g

M_T total mass in the combustion chamber/gun tube, g

p_1 pressure in the liquid reservoir, MPa

p_3 pressure in the combustion chamber, MPa

V_L volume of the liquid in the combustion chamber/gun tube, cm^3

V_G volume of the gas in the combustion chamber/gun tube, cm^3

V_T total volume of the combustion chamber/gun tube, cm^3

γ ratio of specific heats

ρ_1 density of the liquid in the reservoir, g/cm^3

ρ_3 density of the gas in the combustion chamber, g/cm^3

DISTRIBUTION LIST

No. of Copies	Organization
12	Commander Defense Technical Info Center ATTN: DTIC-DDA Cameron Station Alexandria, VA 22304-6145
1	Director Defense Advanced Research Projects Agency ATTN: H. Fair 1400 Wilson Boulevard Arlington, VA 22209
1	HQDA DAMA-ART-M Washington, DC 20310
1	Commander US Army Materiel Command ATTN: AMCDR-ST 5001 Eisenhower Avenue Alexandria, VA 22333-0001
3	Commander Armament R&D Center US Army AMCCOM ATTN: SMCAR-TSS SMCAR-SCA, B. Brodman R. Yalamanchili Dover, NJ 07801
9	Commander Armament R&D Center US Army AMCCOM ATTN: SMCAR-LCA, D. Downs A. Beardell SMCAR-LCE, N. Slagg SMCAR-LCS, W. Quine A. Bracuti J. Lannon R. Price L. Frauen H. Liberman Dover, NJ 07801
3	Director Benet Weapons Laboratory Armament R&D Center US Army AMCCOM ATTN: SMCAR-LCB-TL P. Votis A. Graham Watervliet, NY 12189
1	Commander US Army Armament, Munitions and Chemical Command ATTN: SMCAR-ESP-L Rock Island, IL 61299
1	Commander US Army Aviation Research and Development Command ATTN: AMSAV-E 4300 Goodfellow Blvd. St. Louis, MO 63120
1	Director US Army Air Mobility Rsch. and Development Lab. Ames Research Center Moffett Field, CA 94035
1	Commander US Army Communications Electronics Command ATTN: AMSEL-ED Fort Monmouth, NJ 07703
1	Commander ERADCOM Technical Library ATTN: DELSD-L (Reports Section) Ft. Monmouth, NJ 07703-5301
1	Commander US Army Harry Diamond Labs ATTN: DELHD-TA-L 2800 Powder Mill Rd Adelphi, MD 20783

DISTRIBUTION LIST

No. of Copies	Organization
1	Commander US Army Missile Command Rsch, Dev, & Engr Ctr ATTN: AMSMI-RD Redstone Arsenal, AL 35898
1	Commander US Army Missile & Space Intelligence Center ATTN: AIAMS-YDL Redstone Arsenal, AL 35898-5500
1	Commander US Army Belvoir R&D Ctr ATTN: STRBE-WC Tech Library (Vault) B-315 Fort Belvoir, VA 22060-5606
1	Commander US Army Tank Automotive Cmd ATTN: AMSTA-TSL Warren, MI 48397-5000
1	Commander US Army Research Office ATTN: Tech Library P.O. Box 12211 Research Triangle Park,NC 27709-2211
1	Director US Army TRADOC Systems Analysis Activity ATTN: ATAA-SL White Sands Missile Range NM 88002
1	Commandant US Army Infantry School ATTN: ATSH-CD-CSO-OR Fort Benning, GA 31905
1	Commander US Army Development and Employment Agency ATTN: MODE-TED-SAB Fort Lewis, WA 98433

No. of Copies	Organization
1	Commander Naval Surface Weapons Center ATTN: Code G33, J. East Dahlgren, VA 22448
2	Commander US Naval Surface Weapons Ctr. ATTN: O. Dengel K. Thorsted Silver Spring, MD 20910
1	Commander Naval Weapons Center China Lake, CA 93555-6001
1	Commander Naval Ordnance Station ATTN: C. Dale Code 5251 Indian Head, MD 20640
1	Superintendent Naval Postgraduate School Dept of Mechanical Eng. ATTN: Code 1424, Library Monterey, CA 93943
1	AFWL/SUL Kirtland AFB, NW 87117
1	Air Force Armament Lab ATTN: AFATL/DLODL Eglin, AFB, FL 32542-5000
1	AFOSR/NA (L. Caveny) Bldg. 410 Bolling AFB, DC 20332
1	US Bureau of Mines ATTN: R.A. Watson 4800 Forbes Street Pittsburgh, PA 15213
1	Director Jet Propulsion Lab ATTN: Tech Libr 4800 Oak Grove Drive Pasadena, CA 91109

DISTRIBUTION LIST

No. of Copies	Organization
2	Director National Aeronautics and Space Administration ATTN: MS-603, Tech Lib MS-86, Dr. Povinelli 21000 Brookpark Road Lewis Research Center Cleveland, OH 44135
1	Director National Aeronautics and Space Administration Manned Spacecraft Center Houston, TX 77058
10	Central Intelligence Agency Office of Central Reference Dissemination Branch Room GE-47 HQS Washington, DC 20502
1	Central Intelligence Agency HQ Room 5F22 Washington, D.C. 20505
3	Bell Aerospace Textron ATTN: F. Boorady K. Berman A.J. Friona Post Office Box One Buffalo, NY 14240
1	The BDM Corporation ATTN: Dr. T.P. Goddard P.O. Box 2019 2600 Cearden Rd, North Bldg Monterey, CA 93940
1	Calspan Corporation ATTN: Tech Library P.O. Box 400 Buffalo, NY 14225
1	Commander Armament R,D&E Center U.S. Army AMCCOM ATTN: SMCAR-TDC Dover, NJ 07801
4	General Electric Ord. Sys Dpt ATTN: J. Mandzy, OP43-220 R.E. Mayer H. West M. Bulman 100 Plastics Avenue Pittsfield, MA 01201-3698
1	General Electric Company Armanent Systems Department ATTN: D. Maher Burlington, VT 05401
1	IITRI ATTN: Library 10 W. 35th St. Chicago, IL 60616
1	Olin Chemicals ATTN: Dr. Ronald L. Dotson P.O. Box 248 Charleston, TN 37310
1	Olin Chemicals Research ATTN: David Gavin P.O. Box 586 Chesire, CT 06410-0586
1	Olin Corporation ATTN: Victor A. Corso P.O. Box 30-9644 New Haven, CT 06536
1	Paul Gough Associates ATTN: Paul Gough PO Box 1614 Portsmouth, NH 03801
1	Safety Consulting Engr ATTN: Mr. C. James Dahn 5240 Pearl St. Rosemont, IL 60018
1	Science Applications, Inc. ATTN: R. Edelman 23146 Cumorah Crest Woodland Hills, CA 91364

DISTRIBUTION LIST

No. of Copies	Organization
1	Sunstrand Aviation Operations ATTN: Dr. Owen Briles P.O. Box 7002 Rockford, IL 61125
1	Veritay Technology, Inc. ATTN: E. B. Fisher 4845 Millersport Highway, P.O. Box 305 East Amherst, NY 14051-0305
1	Director Applied Physics Laboratory The Johns Hopkins Univ. Johns Hopkins Road Laurel, Md 20707
2	Director Chemical Propulsion Info Agency The Johns Hopkins Univ. ATTN: T. Christian Tech Lib Johns Hopkins Road Laurel, MD 20707
2	University of Delaware Department of Chemistry ATTN: Mr. James Cronin Professor Thomas Brill Newark, DE 19711
1	U. of ILL. at Chicago ATTN: Professor Sohail Murad Dept of Chemical Eng Box 4348 Chicago, IL 60680
1	U. of MD at College Park ATTN: Professor Franz Kasler Department of Chemistry College Park, MD 20742
1	U. of MO at Columbia ATTN: Professor R. Thompson Department of Chemistry Columbia, MO 65211
1	U. of MO at Columbia ATTN: Professor F. K. Ross Research Reactor Columbia, MO 65211
1	U. of MO at Kansas City Department of Physics ATTN: Prof. R.D. Murphy 1110 East 48th Street Kansas City, MO 64110-2499
1	Pennsylvania State University Dept. of Mechnical Eng ATTN: K. Kuo University Park, PA 16802
2	Princeton Combustion Rsch Laboratories, Inc. ATTN: N.A. Messina M. Summerfield 475 US Highway One North Monmouth Junction, NJ 08852
1	University of Arkansas Department of Chemical Engineering ATTN: J. Havens 227 Engineering Building Fayetteville, AR 72701

Aberdeen Proving Ground

Dir, USAMSAA
ATTN: AMXSY-D
AMXSY-MP, H. Cohen

Cdr, USATECOM
ATTN: AMSTE-TO-F

CDR, CRDC, AMCCOM
ATTN: SMCCR-RSP-A
SMCCR-MU
SMCCR-SPS-IL

USER EVALUATION SHEET/CHANGE OF ADDRESS

This Laboratory undertakes a continuing effort to improve the quality of the reports it publishes. Your comments/answers to the items/questions below will aid us in our efforts.

1. BRL Report Number_____ Date of Report_____

2. Date Report Received_____

3. Does this report satisfy a need? (Comment on purpose, related project, or other area of interest for which the report will be used.)_____

4. How specifically, is the report being used? (Information source, design data, procedure, source of ideas, etc.)_____

5. Has the information in this report led to any quantitative savings as far as man-hours or dollars saved, operating costs avoided or efficiencies achieved, etc? If so, please elaborate._____

6. General Comments. What do you think should be changed to improve future reports? (Indicate changes to organization, technical content, format, etc.)

_____

_____

_____

CURRENT ADDRESS

_____
Name

_____
Organization

_____
Address

_____
City, State, Zip

7. If indicating a Change of Address or Address Correction, please provide the New or Correct Address in Block 6 above and the Old or Incorrect address below.

OLD ADDRESS

_____
Name

_____
Organization

_____
Address

_____
City, State, Zip

(Remove this sheet along the perforation, fold as indicated, staple or tape closed, and mail.)

FOLD HERE

Director
U.S. Army Ballistic Research Laboratory
ATTN: SLCBR-DD-T
Aberdeen Proving Ground, MD 21005-5066

NO POSTAGE
NECESSARY
IF MAILED
IN THE
UNITED STATES

OFFICIAL BUSINESS
PENALTY FOR PRIVATE USE, $300

BUSINESS REPLY MAIL
FIRST CLASS PERMIT NO 12062 WASHINGTON, DC
POSTAGE WILL BE PAID BY DEPARTMENT OF THE ARMY

Director
U.S. Army Ballistic Research Laboratory
ATTN: SLCBR-DD-T
Aberdeen Proving Ground, MD 21005-9989

FOLD HERE

END

DTIC

7-86